separations

MDPI

Article

Semi-Pilot Scale Extraction of Pinocembrin and Galangin from *Populus alba* L. × *berolinensis* K. Koch via Enzymatic Pretreatment and Ultrasonication

Ru Zhao, Xiaoli Li, Yazhou Bao, Wenjun Xu, Chen Xu, Rongrong Wang, Tianlan Xia, Tingli Liu * and Ailing Ben *

Nanjing Engineering Research Center for Peanut Genetic Engineering Breeding and Industrialization, School of Food Science, Nanjing Xiaozhuang University, Nanjing 211171, China; 2021044@njxzc.edu.cn (R.Z.)
* Correspondence: liutingli@njxzc.edu.cn (T.L.); benailing@njxzc.edu.cn (A.B.)

Abstract

In this investigation, pinocembrin and galangin were efficiently extracted from the male inflorescence of *Populus alba* L. × *berolinensis* K. Koch through an enzymatic pretreatment–ultrasonic-assisted strategy (EP-UAS), and the feasibility of their pilot-scale application was validated. The optimal parameters (ethanol volume fraction, cellulase dosage, incubation temperature, incubation time, pH, liquid-solid ratio, ultrasonic irradiation power during incubation, duty cycle, ultrasonic irradiation power and time during extraction) affecting pinocembrin and galangin yields were systematically explored. The Box–Behnken design (BBD) results provided optimal parameters for the EP-UAS process. Under the optimal conditions, the actual yields of pinocembrin and galangin were 2158.33 ± 0.13 μg/g and 1257.96 ± 0.06 μg/g, respectively. Stability, recovery and reproducibility were determined under the above optimized conditions to evaluate the proposed EP-UAS method. Moreover, laboratory-scale experimental results revealed that the conditions selected via single-factor and response surface experiments were also applicable to pilot-scale production, facilitating industrialization.

Keywords: male inflorescences of *Populus alba* L. × *berolinensis* K. Koch; ultrasonication; pinocembrin; galangin; semi-pilot scale

Academic Editor: Aleksandra Mišan

Received: 16 August 2025
Revised: 3 September 2025
Accepted: 10 September 2025
Published: 11 September 2025

Citation: Zhao, R.; Li, X.; Bao, Y.; Xu, W.; Xu, C.; Wang, R.; Xia, T.; Liu, T.; Ben, A. Semi-Pilot Scale Extraction of Pinocembrin and Galangin from *Populus alba* L. × *berolinensis* K. Koch via Enzymatic Pretreatment and Ultrasonication. *Separations* **2025**, *12*, 249. https://doi.org/10.3390/separations12090249

1. Introduction

Populus alba L. × *berolinensis* K. Koch was cultivated by the Shelter Forest Research Institute (Heilongjiang, China) in the 1980s, with *Populus alba* L. as the female parent and *Populus berolinensis* K. Koch as the male parent [1]. *P. alba* × *berolinensis* is an excellent heterozygous male poplar clone that is unique and has been widely promoted in fast-growing and high-yield forests in more than 10 provinces and regions including Northeast China, Northwest China and North China, owing to its excellent characteristics like a short growth cycle, fast growth rate, strong overwintering ability, stress resistance and a beautifying environment [2–4]. At present, the application of poplars generally focuses on wood [5], and *P. alba* × *berolinensis* produces many male inflorescences 5 cm in length that fall to the ground in April each year. This not only affects the appearance of cities and human health, but also wastes *P. alba* × *berolinensis* resources.

Many chemical components, such as glycosides, flavanoids and phenols, have been previously identified in the male inflorescences of *Flos populi* [6–8]. Research has shown that the male inflorescence of *Populus tomentosa* Carrière has a relatively high flavonoid

content, and the contents of several flavonoids including apigenin, pinocembrin, galangin and chrysin have been determined via HPLC [9,10]. Therefore, we inferred that the flavonoids pinocembrin or galangin may be the major components contributing to the active effects of the male inflorescences of *P. alba* × *berolinensis*. The structures of pinocembrin and galangin are presented in Figure 1. Some studies have indicated that pinocembrin (5,7-dihydroxyflavanone) [11], a natural flavonoid, has various biological and pharmacological activities, including antibacterial, antithrombotic, anti-inflammatory and anticancer activities [12,13]. Galangin (3,5,7-trihydroxyflavone) has recently attracted much attention because of its prominent nontoxicity and pharmacological activities [14], including antiviral, antiobesogenic, antimicrobial, anthypolipidemic, antioxidant, anticancer, inflammatory response modulator and vasorelaxant properties [15–18].

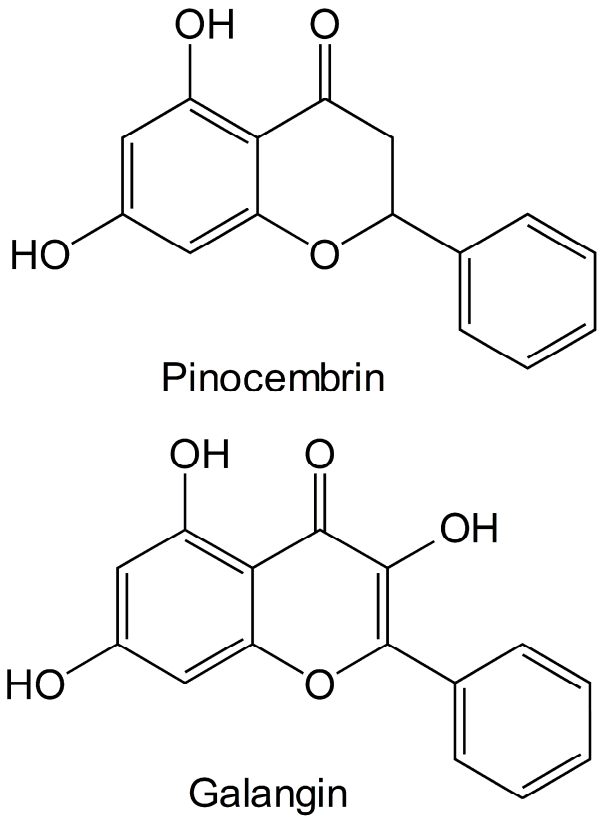

Figure 1. The molecular structures of pinocembrin and galangin.

Currently, conventional methods for extracting these active ingredients include solvent extraction, maceration, heat reflux extraction and percolation, but these methods usually have complex operating conditions, high costs, and long durations, in addition to resulting in incomplete extraction and potentially causing environmental pollution [19]. Additionally, several advanced techniques have been employed such as supercritical fluid extraction [20], ultrasonic-assisted extraction [21], microwave-assisted extraction [22], enzymatic hydrolysis [23] and accelerated solvent extraction [24]. Enzymatic hydrolysis requires prolonged processing times and suffers from incomplete hydrolysis due to the poor permeability of cellulase, a macromolecular enzyme. In contrast, studies have demonstrated that ultrasound-assisted extraction represents an efficient and innovative approach for isolating various bioactive components [7,25,26]. This technique offers significant advantages including operational simplicity, reduced extraction time, lower solvent consumption, energy efficiency, higher extraction yields and environmental friendliness.

The plant cell wall includes cellulose, hemicellulose and pectin, which hinder the release and dissolution of small-molecule target compounds. Therefore, combining enzy-

matic hydrolysis with ultrasonic extraction may serve as an effective strategy for enhancing the extraction of these target components. Cellulase hydrolyzes and cleaves the glycosidic bonds of polysaccharide macromolecules and flavonoid glycosides, facilitating the extraction and dissolution of small-molecule target compounds. Simultaneously, cellulase hydrolyzes flavonoid glycosides into their corresponding aglycones, significantly increasing the yield of the desired components. Moreover, enzymatic methods can effectively disrupt the cell wall, offering several advantages including high reaction sensitivity under low-temperature and -atmospheric-pressure conditions, mild processing requirements, reduced energy consumption and the generation of numerous high-value products [27].

On the basis of previous studies, most combined ultrasonication–enzymatic extraction methods use organic solvents, followed by supernatant filtration after enzymatic hydrolysis and the direct quantification of target components in the supernatant [28]. Water, as the most ideal "green solvent", has been employed for extracting polyphenols, flavonoids and other bioactive compounds, thus reducing environmental pollution and potential safety concerns [29]. However, owing to their varying physicochemical properties, the limited water solubility of many bioactive compounds restricts the broader application of aqueous solvents in green separation processes [30]. For example, flavonoid aglycones exhibit poor water solubility, resulting in incomplete extraction from plant residues. In contrast, organic solvents such as ethanol are more effective at extracting low-molecular-weight components, including flavonoid aglycones. Nevertheless, enzymatic catalysis primarily occurs in the aqueous phase, and ethanol addition can lead to enzyme deactivation. Thus, subsequent ethanol extraction is often required to recover residual target compounds from the solid matrix.

The purpose of this study was to develop an efficient enzymatic pretreatment–ultrasonic-assisted strategy (EP-UAS) technique for extracting pinocembrin and galangin from the male inflorescences of *P. alba* × *berolinensis*. The optimal parameters affecting pinocembrin and galangin yields were systematically studied. Parameters including the linearity, limit of detection (LOD), limit of quantification (LOQ), reproducibility, stability, recovery and precision (intra-day precision and inter-day precision) were determined under the optimized conditions to evaluate the proposed EP-UAS approach, HPLC apparatus and quantitative conditions. Moreover, a pilot-scale experiment was subsequently performed under optimized conditions to verify the feasibility of the proposed EP-UAS technology.

2. Materials and Methods

2.1. Raw Materials and Reagents

Male inflorescences of *P. alba* × *berolinensis* were collected in April 2024 from Harbin, Heilongjiang Province, China. The botanical identification was performed by Prof. Ailing Ben (Nanjing Xiaozhuang University, China). The plant specimen was stored in the herbarium of Key Construction Laboratories of Provincial Universities for the Resource Utilization of Food and Drug Substances (specimen number: PB20240401). The morphological characteristics of the male inflorescences are presented in Figure 2. The materials were dried in an oven at 80 °C for 24 h before being crushed, and the moisture content was measured below 5%. Prior to experimentation, the raw materials were homogenized via a mechanical disintegrator and subsequently filtered through a 60-mesh sieve. The powdered samples were stored in airtight containers under cool, dry conditions for subsequent analyses. The moisture content of the processed inflorescences was determined to be 6.59% (*w*/*w*). Authentic standards of pinocembrin and galangin (purity > 98%) were obtained from Yuanye (Shanghai, China). Analytical-grade methanol, phosphoric acid, and ethanol were procured from Aladdin (Shanghai, China). All the samples were filtered before qualitative and quantitative HPLC analysis.

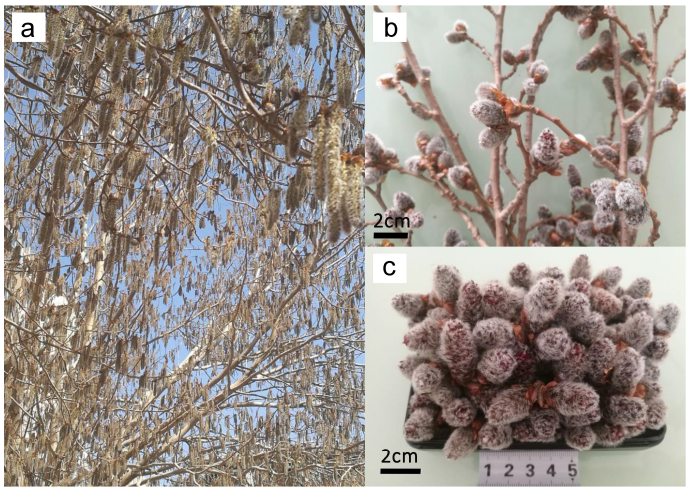

Figure 2. Physical maps of the male inflorescences of *Populus alba* × *berolinensis*, *P. alba* × *berolinensis* (**a**), the male inflorescences of *Populus alba* × *berolinensis* (**b**,**c**).

2.2. Ultraviolet Full-Wavelength Scanning of Standard/Reference Stock Solutions

The pinocembrin and galangin standard solutions were prepared at a concentration of 1.00 mg/mL and then placed in a 4 °C refrigerator. The two standard solutions were subsequently diluted 25 times for full-wavelength scanning via a Cary 100 ultraviolet and visible spectrophotometer (Agilent Technologies, Santa Clara, CA, USA). The full-wavelength scanning results are shown in Figure 3b. They were then detected at wavelengths of 289 nm (pinocembrin) and 270 nm (galangin).

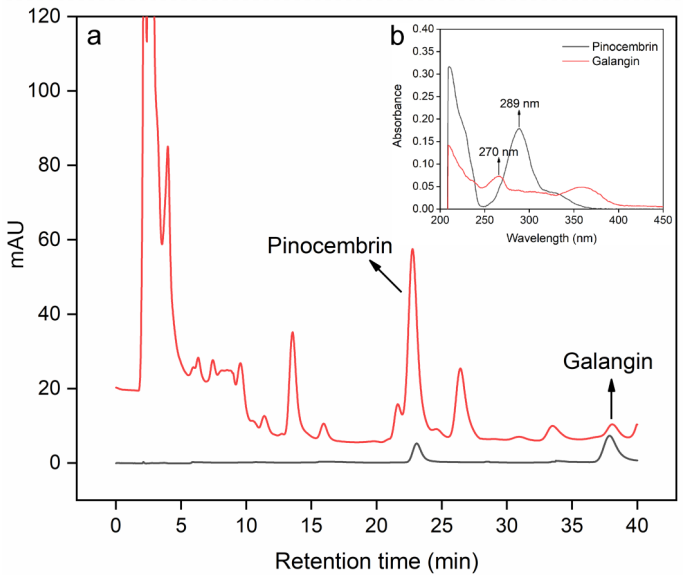

Figure 3. HPLC results for pinocembrin and galangin in the extraction solution (**a**). Insert: UV full-wavelength scanning of pinocembrin and galangin (**b**).

2.3. HPLC Apparatus and Quantitative Conditions

An Agilent 1260 Chromatography System (Agilent Technologies, Santa Clara, CA, USA) was used to determine the pinocembrin and galangin contents. The detailed determination followed Chen's method [31]. The HPLC chromatograms of pinocembrin and galangin are presented in Figure 3. Pinocembrin and galangin were separated at 23.06 min and 37.86 min, respectively.

2.4. Enzymatic Pretreatment-Ultrasonic-Assisted Strategy

2.4.1. Laboratory-Scale Process

The laboratory-scale extraction process was performed via a KQ-250DB ultrasonic bath coupled with a constant-temperature oscillating water bath (Kunshan Shumei Ultrasonic Instrument Co., Ltd., Kunshan, China). The EP-UAS diagram showing the stages of the entire process is presented Figure S1. Specifically, 0.5 g powder was weighed into a 25 mL conical centrifuge tube, followed by the addition of a predetermined volume of cellulase solution. The enzymatic hydrolysis was conducted under controlled temperature and duration conditions, with intermittent ultrasonication applied at specified duty cycles. Following hydrolysis, the reaction mixture was immediately filtered, and the filtrate volume was recorded. The residual solid material was subsequently subjected to ethanol extraction, where absolute ethanol was added to achieve the desired final concentration. Ultrasonic-assisted extraction was then performed for a predetermined time period. The combined extracts were homogenized, filtered and stored at 4 °C for the quantification of pinocembrin and galangin.

2.4.2. Semi-Pilot Scale Process

A semi-pilot-scale ultrasonic extractor device (TGCXN-2B, Beijing Hongxianglong Biotechnology Co., Ltd., Beijing, China) was used in the extraction experiments to achieve industrial production. The equipment configuration follows the schematic representation provided in Chen's study [31]. The equipment has a volume of 2 L and a motor power of 2 kW. The maximum ultrasonic irradiation power was 1200 W (ultrasonic power density 2.08 W/g). The raw materials were expanded 200 times at the semi-pilot scale according to the previous study [32]; 100 g powder of male inflorescences of *P. alba* × *berolinensis* per batch was placed in an ultrasonic container for extraction, and the material-liquid ratio was consistent with that used in the laboratory experiments.

2.5. Box–Behnken Design of the RSM

Preliminary single-factor experiments informed the implementation of a Box–Behnken design (BBD) to optimize extraction parameters and predict optimal yield conditions. With the Design Expert 8.0 software, we employed three-level, three-factor response surface methodology (RSM) to analyze variable interactions and optimize process conditions. Key experimental parameters, including the dose of cellulase (X_1: 10, 25, and 40 mg/g), incubation temperature (X_2: 40, 50, and 60 °C) and incubation time (X_3: 90, 120, and 150 min), were selected for BBD to investigate their interaction influence on the yield of pinocembrin and galangin. The yields of pinocembrin and galangin served as response variables.

2.6. Method Validation

The developed EP-UAS method and HPLC quantitative conditions still need to be validated. The specific method validation parameters were determined according to previous methods [32,33]. Stability and recovery studies of pinocembrin and galangin were conducted using male inflorescence samples of *P. alba* × *berolinensis* powder extracted under optimized conditions. Reproducibility was evaluated through quintuplicate analyses (0.5 g samples per replicate).

3. Results and Discussion

3.1. Effect of the Ethanol Volume Fraction

As one of the major factors affecting the yields of pinocembrin and galangin, the ethanol volume fraction varied from 0% to 90% in this study, while the other experimental conditions were kept the same (cellulase dosage of 25 mg/mL, incubation temperature of 45 °C, incubation time of 150 min, pH of 5, liquid-solid ratio of 20 mL/g, ultrasonic

irradiation power during incubation of 200 W, duty cycle of 16.67%, ultrasonic irradiation power and time during extraction of 200 W and 10 min). Figure 4 shows that when it ranged from 0% to 70%, the pinocembrin and galangin yields increased gradually. In contrast, the yields decreased with increasing ethanol volume fraction, suggesting that 70% may be a suitable concentration for extracting pinocembrin and galangin. The same trends have also been reported in other studies on different ethanol volume fractions for the extraction of flavonoids [34]. This observation indicates that 70% ethanol enhanced the extraction efficiency of the two compounds from *P. alba* × *berolinensis* male inflorescences compared with the other volume fractions. Ethanol can lower the dielectric constant of the extraction solvent, thereby improving component solubility and mass transfer [35].

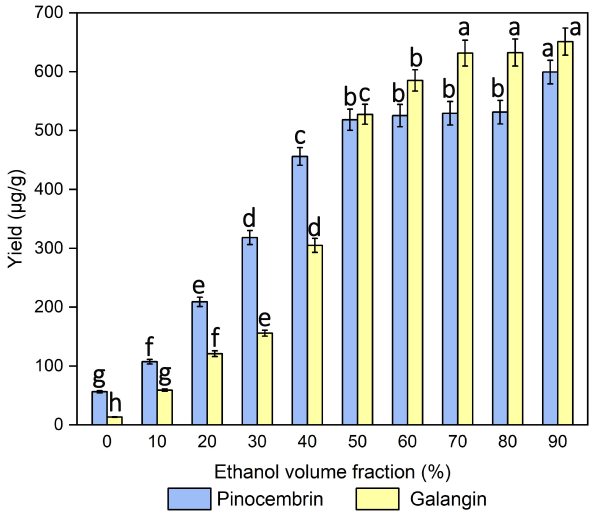

Figure 4. Effect of the ethanol volume fraction on the extraction yields of pinocembrin and galangin, values with different letters are significantly different ($p < 0.05$).

Moreover, when the ethanol volume fraction was relatively low, the yields of pinocembrin and galangin were lowest, at only 53.36 and 13.44 μg/mL, respectively, when the volume fraction was 0. Sandra M. reported a similar phenomenon in which flavonoid extraction (orientin) from *Passiflora quadrangularis* leaves was detected in all hydroalcoholic extracts, but was not detected previously in aqueous extracts [10]. However, a higher ethanol volume fraction also resulted in a lower extraction efficiency. This effect could be attributed to the poor water solubility of pinocembrin and galangin, where higher ethanol concentrations induced cellular dehydration and protein denaturation, thereby hindering component diffusion. Additionally, water promoted plant material swelling, substantially increasing the matrix-solvent contact area. The surface tension and viscosity of the solvent also play crucial roles in cavitation dynamics during ultrasound-assisted extraction [36]. Finally, the relative polarity of 70% ethanol promoted the extraction of pinocembrin and galangin, and was selected.

3.2. Effects of the Dose of Cellulase

The extraction of different doses of cellulase (0, 5, 10, 25, 50, and 100 mg/g materials) was investigated, while the other experimental conditions were kept the same. As shown in Figure 5a, within a certain range of doses of cellulose (0–25 mg/g), the pinocembrin and galangin yields gradually increased, and the extraction efficiency was the highest when the dose of cellulase was 25 mg/mL. As the dose of cellulase increased, the extraction efficiency basically remained unchanged. In addition, the yields of pinocembrin and galangin were only 1009 and 292.26 μg/mL, respectively, when the dose of cellulase was 0, which values are 557.92 and 542.45 μg/mL lower than the 25 mg/g dose of cellulase. As an essential structural element of the primary cell walls of male inflorescences of *P. alba* × *berolinensis*, cellulose

can be decomposed by cellulase at suitable temperatures and pH values [37,38]. The results demonstrate that a cellulase concentration of 25 mg/mL optimized the extraction efficiency for pinocembrin and galangin. Accordingly, a liquid-to-solid ratio of 25 mL/g was selected for further processing to minimize solvent consumption and operational expenses.

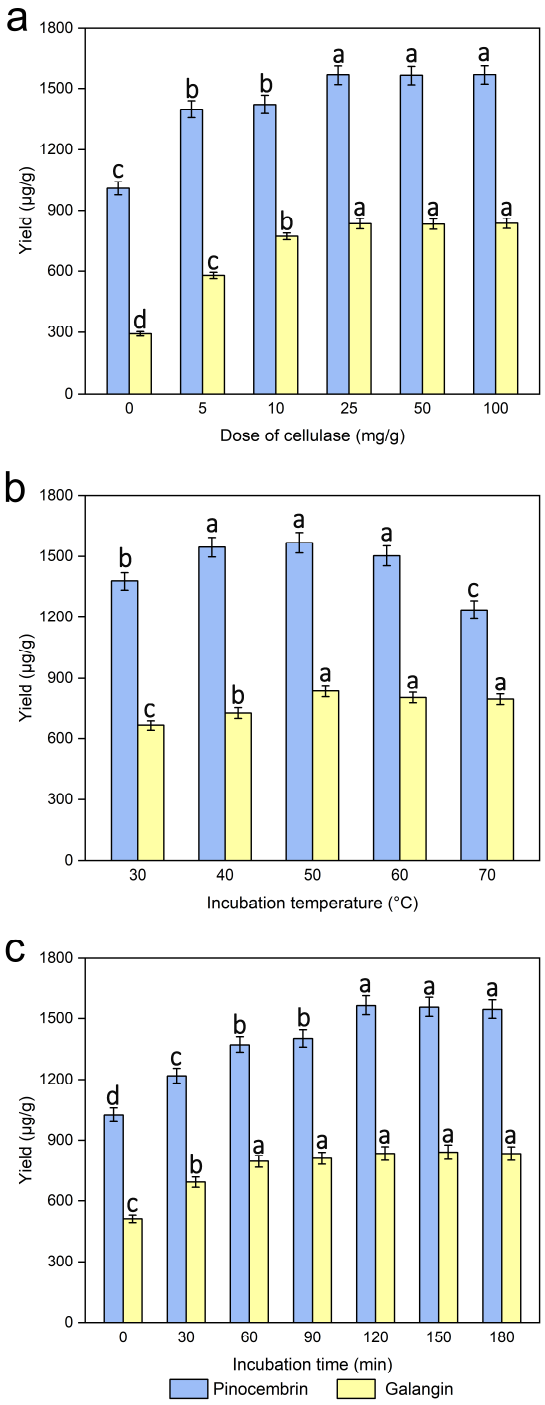

Figure 5. Effect of the dose of cellulase (**a**), incubation temperature (**b**), and incubation time (**c**) on the extraction yields of pinocembrin and galangin, values with different letters are significantly different ($p < 0.05$).

3.3. Effect of the Incubation Temperature

The incubation temperature, which is a critical element affecting the activity of cellulase used in the enzymatic hydrolysis process, was necessary to ensure efficient extraction. The extraction of incubation temperature (30, 40, 50, 60, 70 °C) was investigated, while the other

experimental conditions were kept the same. The results shown in Figure 5b reveal that at an opposite range of incubation temperatures (30–50 °C), a gradual increase in pinocembrin and galangin was observed, and their yields reached a maximum plateau at 50 °C. The dissolution of the target extract could be accelerated, and its viscosity could be reduced at higher temperatures, which accelerated the entire enzymatic hydrolysis process. Instead, the yield gradually decreased with increasing temperature, i.e., the incubation temperature was greater than 50 °C. The observed effect likely stems from elevated temperatures promoting flavonoid degradation (oxidation) or isomerization, because higher temperatures may increase degradation and thus decrease the extraction yield [39]. Furthermore, a relatively high incubation temperature would cause the cellulase or substrate to become denatured and inactive, thus affecting the results. A similar result was reported when arabinoxylan was extracted from wheat bran via ultrasound-assisted enzymatic hydrolysis extraction at different temperatures [40]. In conclusion, an incubation temperature of 50 °C was chosen.

3.4. Effect of Incubation Time

A series of experiments were carried out with different incubation times (0, 30, 60, 120, 150, and 180 min) to examine the effect of incubation time on pinocembrin and galangin extraction efficiency, while the other experimental conditions were kept the same. Figure 5c shows a significant increase in pinocembrin and galangin contents with increasing incubation time (0–120 min), beyond which the yield did not obviously change with increasing incubation time. A marked increase in pinocembrin and galangin was detected at 30 min, and the yield reached a maximum plateau at 120 min. A longer incubation time can provide sufficient time for ensuring that cellulase thoroughly hydrolyzes the cell wall. Therefore, 120 min would be an appropriate incubation time for use in the following experiments.

3.5. Effect of pH

pH was investigated by extracting the male inflorescences of *P. alba* × *berolinensis* powders at various pH values (4.0, 4.5, 5.0, 5.5, and 6.0), while the other experimental conditions were kept unchanged. In general, changes in pH cause the ionization of enzymes, and then have various degrees of impact on their activity and structure because each enzyme has a specific pH optimum. Figure 6a showed that the yields of pinocembrin and galangin improved slightly as the pH increased, and the yield reached a maximum when the pH was 5. However, a slight reduction in yield was observed as the pH continued to increase. It was speculated that pH could affect the total net charge of enzymes. Optimal pH control during enzymatic hydrolysis is essential for effective cell wall disruption and maximal pinocembrin and galangin production, and suboptimal pH may cause enzyme deactivation or protein denaturation [41]. Thus, a pH of 5 was a good choice.

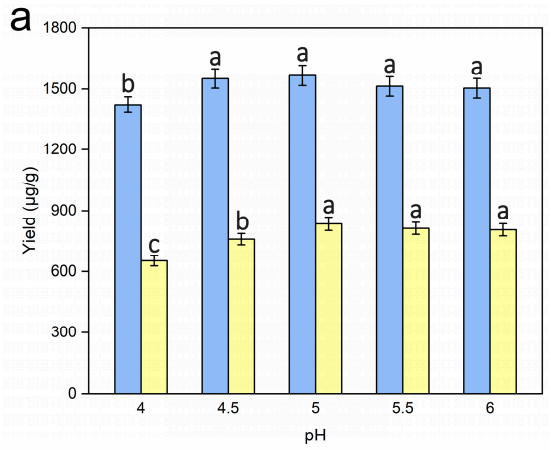

Figure 6. *Cont.*

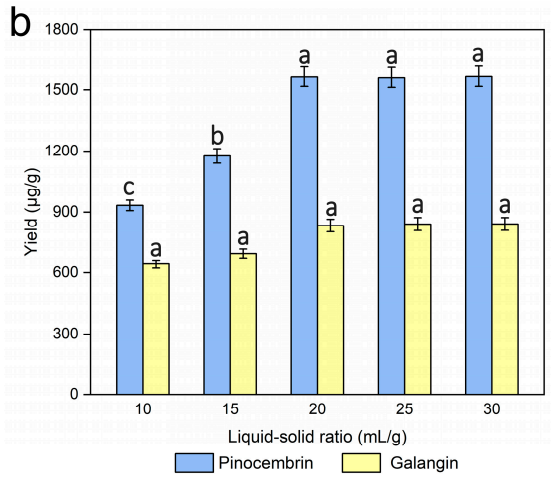

Figure 6. Effects of pH (**a**) and the liquid-solid ratio (**b**) on the extraction yields of pinocembrin and galangin, values with different letters are significantly different ($p < 0.05$).

3.6. Effects of the Liquid-Solid Ratio

Several experiments on the effects of different liquid-solid ratios (10, 15, 20, 25, and 30 mL/g) on pinocembrin and galangin were carried out, while the other experimental conditions were kept unchanged. As shown in Figure 6b, the yields of pinocembrin and galangin rapidly improved in the range of 10–20 mL/g liquid-solid ratios, and subsequently increased slightly as the liquid-solid ratio increased. Some similar trends have also been presented in several studies [40,42], although the optimal value of the liquid-solid ratio varies. Usually, a lower solvent volume contributes to insufficient extraction, which leads to a reduction in the yield of pinocembrin and galangin. Nevertheless, when the liquid-solid ratio exceeds a certain range of values, the sample and solvent are not mixed sufficiently because more solid particles exist in the solution and might adsorb more solvent, resulting in lower extraction yields [42]. Considering both the consumption of the experimental materials and the yields of pinocembrin and galangin, a liquid-solid ratio of 20 mL/g was adopted as the ideal condition for extraction.

3.7. Effects of the Ultrasound Irradiation Power on the Incubation Process

The ultrasonic irradiation power used in the incubation process is also a critical factor affecting the enzymatic hydrolysis process, and several tests were performed with different ultrasonic irradiation powers (100, 150, 200, and 250 W), while the other experimental conditions were kept unchanged. Figure 7a shows that the yields of pinocembrin and galangin were at their maximum when the ultrasonic irradiation power was 200 W. A higher ultrasonic irradiation power was beneficial for increasing the degradation of the cell walls of *P. alba* × *berolinensis*, which may be the major cause of the higher extraction yields of pinocembrin and galangin.

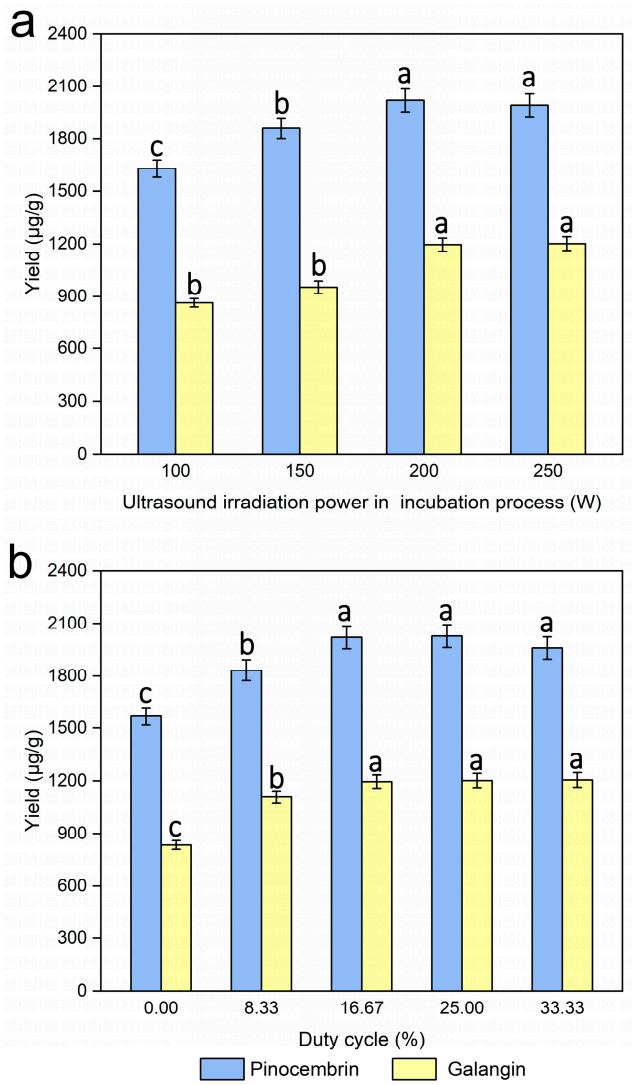

Figure 7. Effects of ultrasound irradiation power during the incubation process (**a**) and duty cycle (**b**) on the extraction yields of pinocembrin and galangin, values with different letters are significantly different ($p < 0.05$).

3.8. Effect of the Duty Cycle

Pinocembrin and galangin yields were evaluated under various duty cycles (0%, 8.33%, 16.77%, 25.00% and 33.33%) to assess operational parameter effects, while the other experimental conditions were kept unchanged. Figure 7b shows that, compared with that in the control treatment, a significant increase in the enzymatic hydrolysis process was observed during the cycle treatment. The yields of pinocembrin and galangin were maximized when the duty of the cycle was 16.67. In addition, no obvious change was found in the yields of pinocembrin and galangin as the duty cycle increased further. This effect likely results from enhanced enzymatic hydrolysis rates under ultrasonication, which improved the mass transfer of enzyme macromolecules between the solid and liquid phases [22]. Finally, a duty cycle of 16.67% was considered for the following experiments.

3.9. Effects of Ultrasound Irradiation Power on the Extraction Process

The ultrasonic irradiation power was investigated via the process of extraction under various controlled ultrasonic irradiation powers (0, 100, 150, 200 and 250 W), while the other experimental conditions were kept unchanged. Figure 8a clearly shows that different degrees of ultrasonic irradiation were more conducive to the extraction efficiency of

pinocembrin and galangin than was the control. When increasing the ultrasonic irradiation power from 100 to 250 W, the yields of pinocembrin and galangin increased. Pinocembrin and galangin yields peaked at 200 W, with no significant increase observed at higher ultrasonic power levels, which was attributed to the fact that ultrasonic treatment during the extraction process of pinocembrin and galangin resulted in cavitations and the increased diffusion of the solvent and target ingredients, which may affect the extraction efficiency related to ultrasonic energy output [43], so the ultrasound irradiation power applied in the extraction process for maximum yields of pinocembrin and galangin should be 200 W for the experiments.

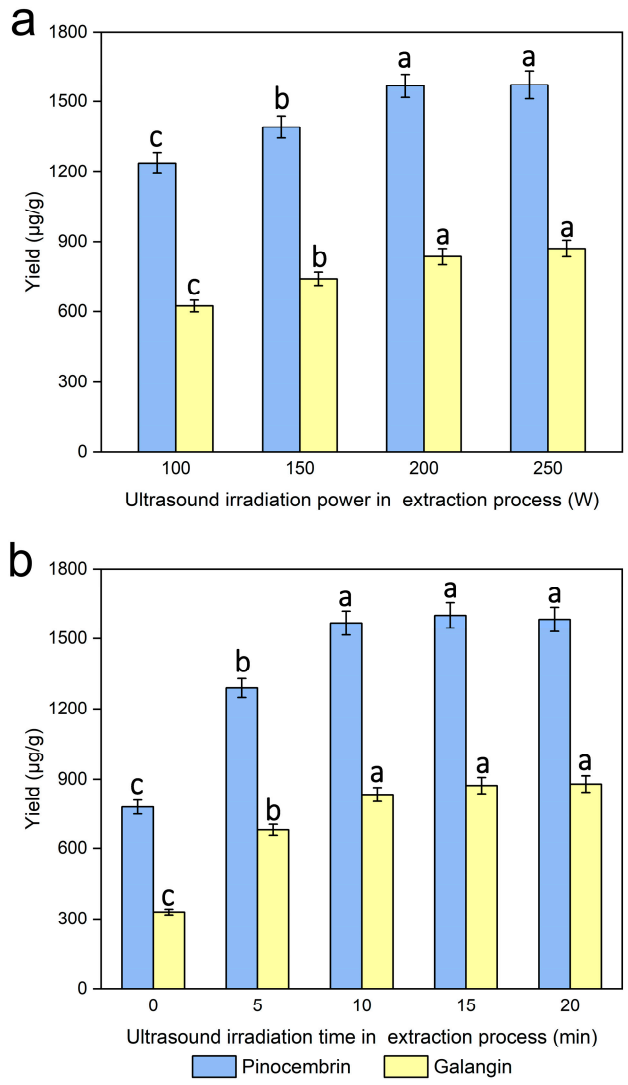

Figure 8. Effect of ultrasonic irradiation power during the extraction process (**a**) and ultrasonic irradiation time during the extraction process (**b**) on the extraction yields of pinocembrin and galangin, values with different letters are significantly different ($p < 0.05$).

3.10. Effect of Ultrasound Irradiation Time on the Extraction Process

The ultrasound irradiation time was evaluated for the extraction of pinocembrin and galangin within the range of 0–20 min, while the other experimental conditions were kept unchanged. Figure 8b revealed that the yield of pinocembrin and galangin increased significantly during the first 10 min of the ultrasonic irradiation process, and subsequently improved with increasing ultrasonic irradiation time. Research has indicated that ultrasonication may increase enzyme activity [44]. In addition, the activity of the enzyme improved, and the diffusion of particles or external solvents into the cells improved with increasing

ultrasound irradiation time during the extraction process, which may have facilitated the release of pinocembrin and galangin from plant cells and their dissolution in the external solvent; consequently, a higher yield was obtained [45,46]. The experimental results reveal that the optimal ultrasonic irradiation time in the extraction process for maximum yields of pinocembrin and galangin should be 15 min for the experiments.

3.11. Parameter Optimization via Response Surface Methodology (RSM)

To optimize the effects of three process parameters (dose of cellulase, incubation temperature, incubation time) on the yields of pinocembrin and galangin, a Box–Behnken design (BBD) combined with RSM was used in the present work. A cellulase dose of 25 mg/g, an incubation temperature of 50 °C, and an incubation time of 120 min were selected as the central conditions of the BBD. The Box–Behnken design (BBD) for the actual experimental values and predicted values for yields of pinocembrin and galangin are presented in Table 1. Table 1 shows that the maximum yields of galangin (1255.93 μg/g) and pinocembrin (2121.71 μg/g) were recorded under the experimental parameters of 25 mg/g cellulase, an incubation temperature of 50 °C and an incubation time of 120 min. The lowest yields of galangin (985.30 μg/g) and pinocembrin (1731.31 μg/g) were observed in the different tests. Moreover, the yields of galangin (1250.17 μg/g) and pinocembrin (2113.03 μg/g) were also high with 40 mg/g cellulase, an incubation temperature of 50 °C, and an incubation time of 150 min, without much variation compared with the highest yield, which contributed to the similar stability of the enzyme within the tested temperature and time range [40].

Table 2 presents the quadratic model's regression coefficients and variance analysis, as determined by the BBD for extracting pinocembrin and galangin. The predicted model F values of Y_1 and Y_2 were 37.73 and 15.43 μg/g, respectively, and their p values were both less than 0.05, which indicats that the model was significant. Lack of fit is an important index used to evaluate the reliability of the equation. The p values of Y_1 and Y_2 for lack of fit were 0.0663 and 0.2940 (>0.05), which implies that this regression equation could effectively describe the relationships between different factors and response values. The factors with p values less than 0.05, such as the linear coefficient (X_2, X_3), interactive coefficient ($X_{2\times3}$), and quadratic coefficient ($X_2{}^2$) were significant in the Y_1 and Y_2 models. The credibility analysis of the regression equations has revealed that the coefficient of determination (R^2) values for the predicted models of Y_1 and Y_2 were 0.9798 and 0.9520, respectively, whereas the adjusted determination coefficient (R^2) values for the predicted models of Y_1 and Y_2 were 0.9538 and 0.8903, respectively, which indicates that the model with the predicted value is reliable, effective, and very suitable for processing the experimental results, and that the experimental and predicted values had high degrees of correlation. "Adeq precision" means the signal-to-noise ratio. The signal-to-noise ratios of Y_1 and Y_2 were 18.28 and 13.22, respectively, which are greater than 4.0, indicating that the obtained signals were adequate, thus presenting the same trend as Yang's study [32].

After the three factors and levels were fitted and analyzed, the multivariate quadratic regression equations between the yields of galangin (Y_1) and pinocembrin (Y_2) and the independent variables of the dose of cellulase (X_1), incubation temperature (X_2), and incubation time (X_3) were obtained as follows:

$$Y_1 = 1248.16 - 10.86\,X_1 - 70.01\,X_2 + 13.09\,X_3 - 19.56\,X_1X_2 + 2.88\,X_1X_3 + 24.02\,X_2\,X_3 - 10.44\,{X_1}^2 - 135.95\,{X_2}^2 + 11.02\,{X_3}^2$$

$$Y_2 = 2095.37 + 25.40\,X_1 - 125.60\,X_2 + 70.89\,X_3 + 56.25\,X_1X_2 + 9.52\,X_1X_3 - 11.29\,X_2\,X_3 - 65.20\,{X_1}^2 - 245.26\,{X_2}^2 + 28.31\,{X_3}^2$$

Table 1. Box–Behnken design (BBD) for the experimental values and predicted values for yields of galangin and pinocembrin.

Run	Factor X_1 Dose of Cellulase (mg/g)	Factor X_2 Incubation Temperature (°C)	Factor X_3 Incubation Time (min)	Response 1 Predicted Galangin Yield (μg/g)	Response 1 Actual Galangin Yield (μg/g)	Response 2 Predicted Pinocembrin Yield (μg/g)	Response 2 Actual Pinocembrin Yield (μg/g)
1	10	40	120	1163.08	1179.63	1941.35	1933.74
2	40	40	120	1180.49	1182.51	1879.66	1927.96
3	10	60	120	1062.18	1060.15	1577.66	1731.31
4	40	60	120	1001.33	985.30	1740.96	1789.15
5	10	50	90	1249.38	1253.05	1971.70	2020.49
6	40	50	90	1221.90	1240.10	2003.47	2000.25
7	10	50	150	1269.80	1251.61	2094.44	2098.57
8	40	50	150	1253.84	1250.17	2164.29	2113.03
9	25	40	90	1204.17	1183.95	1921.84	1985.79
10	25	60	90	1016.11	1014.09	1693.22	1745.77
11	25	40	150	1182.31	1183.95	2086.20	2089.90
12	25	60	150	1090.32	1110.54	1812.42	1855.66
13	25	50	120	1248.16	1250.17	2095.37	2006.03
14	25	50	120	1248.16	1228.58	2095.37	2118.82
15	25	50	120	1248.16	1251.61	2095.37	2121.71
16	25	50	120	1248.16	1254.49	2095.37	2118.82
17	25	50	120	1248.16	1255.93	2095.37	2115.92

Table 2. Estimated regression coefficients and analysis of variance for the response surface quadratic model determined from BBD for galangin and pinocembrin extraction.

Source	Degree of Freedom		Sum of Squares		Mean Square		*F*-Value		*p*-Value [a]	
	Galangin	Pinocembrin	Galangin	Pinocembrin	Galangin	Pinocembrin	Galangin	Pinocembrin	Galangin	Pinocembrin
Model	9	9	124,559	464,642	13,840	51,627	37.73	15.43	<0.0001 *	0.0008 *
X_1	1	1	944	5163	944	5163	2.57	1.54	0.1528	0.2542
X_2	1	1	39,216	126,200	39,216	126,200	106.91	37.71	<0.0001 *	0.0005 *
X_3	1	1	1370	40,202	1370	40,202	3.74	12.01	0.0945	0.0105 *
X_1X_2	1	1	1531	12,655	1531	12,655	4.17	3.78	0.0804	0.0929
X_1X_3	1	1	33	362	33	362	0.09	0.11	0.7724	0.7517
X_2X_3	1	1	2307	510	2307	510	6.29	0.15	0.0405 *	0.7079
X_1^2	1	1	459	17,902	459	17,902	1.25	5.35	0.3002	0.0540
X_2^2	1	1	77,816	253,269	77,816	253,269	212.14	75.67	<0.0001 *	<0.0001 *
X_3^2	1	1	511	3374	511	3374	1.39	1.01	0.2764	0.3488
Residual	7	7	2568	23,428	367	3347				
Lack of fit	3	3	2068	13,317	689	4439	5.52	1.76	0.0663	0.2940
Pure error	4	4	500	10,112	125	2528				
Cor total	16	16	127,127	488,071						

Credibility analysis of the regression equations	Index mark	Standard deviation	Mean	CV%	Press	R^2	Adjust R^2	Predicted R^2	Adequacy precision
	Y_1	19.15	1184.45	1.62	33,866.76	0.9798	0.9538	0.7336	18.28
	Y_2	57.85	1962.59	2.95	228,868.46	0.9520	0.8903	0.5311	13.22

* [a] Significant at $p < 0.05$.

The response surfaces were plotted in the Design Expert software, which demonstrated the influences of three parameters (dose of cellulase, incubation temperature, and incubation time) and their interactions on the yield of galangin and pinocembrin. Figure 9a depicts the interaction effect of dose of cellulase (X_1) and incubation temperature (X_2) on galangin yield, which revealed that these two factors strongly influence the yield of galangin and the curvature of the response surface. With increasing doses of cellulase and incubation temperatures, the enzyme reaction rate increased, and the yield of galangin increased significantly. A slight decrease in the yield of galangin was subsequently observed when the dose of cellulase and incubation temperature increased further. Elevated temperatures may induce enzyme denaturation by disrupting tertiary structures, thereby reducing the yield of galangin [40]. Figure 9b shows the interaction effect of the dose of cellulase (X_1) and incubation time (X_3) on the yield of galangin. The galangin yield did not obviously improve even with increasing cellulase dose or incubation time. A higher dose of cellulase and longer incubation time improved the yield of galangin. Figure 9c shows the interaction effect of the incubation temperature (X_2) and incubation time (X_3) on the yield of galangin, as a result of which the yield gradually increased as the incubation temperature increased and the incubation time increased, whereas a significant reduction in the galangin yield was observed as the experiment progressed.

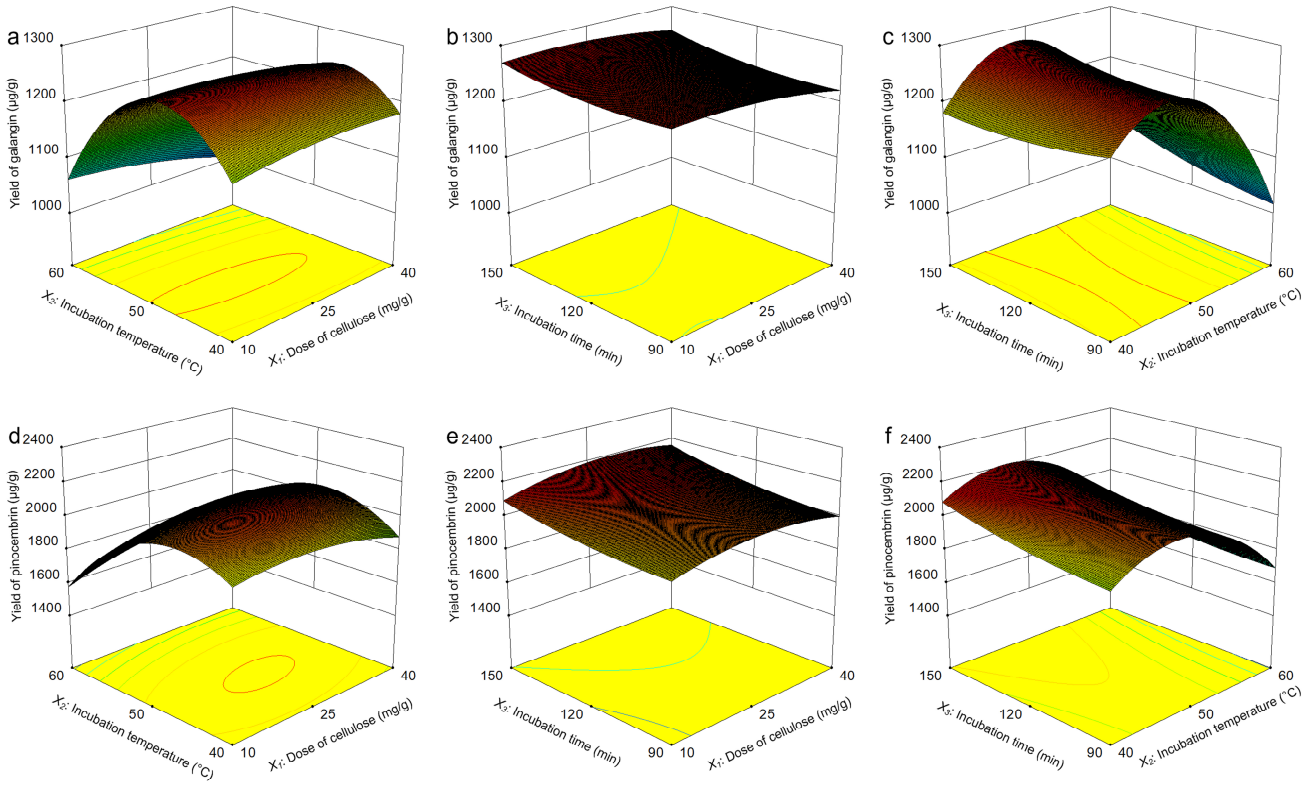

Figure 9. Optimization of yields of pinocembrin and galangin via Box–Behnken design (BBD). Interaction effect of the cellulase dose and incubation temperature on the yield of galangin (**a**); interaction effect of the cellulase dose and incubation time on the yield of galangin (**b**); interaction effect of the incubation temperature and incubation time on the yield of galangin (**c**); interaction effect of the cellulase dose and incubation temperature on the yield of pinocembrin (**d**); interaction effect of the cellulase dose and incubation time on the yield of pinocembrin (**e**); and interaction effect of the incubation temperature and incubation time on the yield of pinocembrin (**f**).

Figure 9d shows the interaction effect of the dose of cellulase (X_1) and incubation temperature (X_2) on the yield of pinocembrin. With increasing cellulase and incubation temperatures, the yield first increased but then decreased, and a similar variation tendency

is presented in Figure 9a. The curves in Figure 9e were plotted to further explain the interaction between two variables, which is similar to the 3D response surface in Figure 9b. The optimum yield was observed at the average dose of cellulase and incubation time without significant effects on the yield of pinocembrin. The yield of pinocembrin is shown as a function of the dose of cellulase (X_1) and incubation temperature (X_2) in Figure 9f. The yield increased with increasing combinations of factors; however, the impact of the incubation temperature was slightly greater than that of the dose of cellulase.

For simultaneous pinocembrin and galangin yield maximization, the model-predicted optimal parameters were as follows: 40 mg/g dose of cellulase, incubation temperature of 46.30 °C, and 147.36 min incubation time. However, for practical convenience, the actual parameter conditions are as follows: 40 mg/g dose of cellulase, 45 °C incubation temperature, and 150 min incubation time. The yields of galangin and pinocembrin predicted by the software were 1259.00 μg/g and 2158.85 μg/g, respectively. Under these conditions, three sets of verification tests were carried out, and the extraction yields of pinocembrin and galangin were 2158.33 ± 0.13 μg/g and 1257.96 ± 0.06 μg/g, respectively.

3.12. Method Validation

The calibration curves of pinocembrin and galangin, namely, the relationships between their peak areas (Y) and concentrations (X), were generated via the standard addition method. The calibration curve regression equation for pinocembrin and galangin was $Y_{\text{pinocembrin}}$ = (2.3054 ± 0.0499) × (0.2693 ± 4.1346) (R^2 = 0.9981, n = 5), Y_{galangin} = (4.6312 ± 0.0614) × (1.9452 ± 5.0787) (R^2 = 0.9993, n = 5), which indicates the good linearity of the calibration curves for pinocembrin and galangin over the range of 0.01–2.50 mg/mL. The limits of detection (LODs) for pinocembrin and galangin were determined to be 0.0036 mg/mL and 0.0059 mg/mL, respectively, while their corresponding limits of quantification (LOQs) were 0.0197 mg/mL and 0.0176 mg/mL, respectively. The stability and recovery studies have demonstrated that the EP-UAS extraction method coupled with HPLC analysis achieved optimal recovery rates for both analytes.

The stability and recovery studies of pinocembrin and galangin standards were evaluated under the following EP-UAS conditions: ethanol volume fraction of 70%, cellulase dosage of 40 mg/mL, incubation temperature of 45 °C, incubation time of 150 min, pH of 5, liquid-solid ratio of 20 mL/g, duty cycle of 16.67%, ultrasonic irradiation power during incubation at 200 W, ultrasonic irradiation power during extraction at 200 W, and ultrasound irradiation time during extraction of 10 min. Table 3 shows that the average recovery of the standard solution of pinocembrin and the recovery of the recovered concentration after 7 days were 99.25% and 97.67%, respectively, whereas the average recovery of the standard solution of galangin and the recovery of the recovered concentration after 7 days were 98.64% and 96.93%, respectively. The results confirm that no thermal isomerization or degradation occurred under the predicted operational parameters.

Method accuracy was assessed by spiking male inflorescences of *P. alba* × *berolinensis* samples with pinocembrin and galangin standard solutions at low, medium and high concentrations, followed by HPLC analysis. The measured pinocembrin and galangin contents were used to calculate recovery rates, which were 99.15% and 98.93%, respectively, as shown in Table 3, confirming the accuracy of the method. Method precision was confirmed by intraday and interday assays (RSD < 2%). Detailed precision data are provided in Table 3, which support the reproducibility of the method.

Table 3. Method validation studies.

Stability studies of pinocembrin and galangin standards under the following EP-UAS [a] conditions: ethanol volume fraction of 70%, cellulase dosage of 40 mg/mL, incubation temperature of 45 °C, incubation time of 150 min, pH of 5, liquid-solid ratio of 20 mL/g, ultrasonic irradiation power during incubation of 200 W, duty cycle of 16.67%, ultrasonic irradiation power during extraction of 200 W and ultrasonic irradiation time during extraction of 10 min.								
Compounds	Initial concentration (mg/mL)	Recovered concentration after EP-UAS (mg/mL)		RSD% (n = 3)	Average recovery (%)	Recovered concentration after 7 days (mg/mL)	RSD% (n = 3)	Average recovery (%)
Pinocembrin	0.1090	0.1080		0.98	99.25	0.1065	0.99	97.67
Galangin	0.1091	0.1082		0.97	98.64	0.1060	0.96	96.93
Recovery of pinocembrin and galangin from the male inflorescences of *Populus alba* × *berolinensis*								
Sample		Content of the sample (mg)		Mass of added standard (mg)		Mass of the sample analyzed with added standard (mg)		Recovery (%)
		Pinocembrin	Galangin	Pinocembrin	Galangin	Pinocembrin	Galangin	Pinocembrin Galangin
1		1.25	2.31	0.50	2.00	1.64	4.82	99.74 99.86
2		1.25	2.31	1.00	3.00	2.13	5.78	99.26 98.72
3		1.25	2.31	1.50	4.00	2.61	6.75	98.45 98.23
Average								99.15 98.93
Precision results as peak area of different determinations on 3 different days (pinocembrin 0.1090 mg/mL, galangin 0.1091 mg/mL (n = 3), acceptance limit RSD% < 2)								
Sample		Day 1		Day 2		Day 3		
		Pinocembrin	Galangin	Pinocembrin	Galangin	Pinocembrin	Galangin	
1		3688	4042	3636	4021	3617	4015	
2		3680	4016	3621	4016	3602	3956	
3		3566	4010	3510	3927	3524	3892	
Mean		3645	4004	3589	3988	3581	3954	
Standard deviation		68.24	45.21	68.83	52.89	49.93	61.52	
RSD%		1.87	1.13	1.92	1.33	1.39	1.56	

[a] EP-UAS: Enzymatic pretreatment–ultrasonic-assisted strategy.

3.13. Semi-Pilot-Scale Verification Experiment

The literature indicates that ultrasound-assisted extraction is a useful method that is accepted by the industry, and is contributing to the development of small- or large-scale methods in the phytopharmaceutical industry [32]. Therefore, in this study, to evaluate the validity of the EP-UAS technique and scale-up verification tests (taking 100 g of powder, n = 5) in a semi-pilot-scale device, three tests were performed at the optimal state to evaluate the effectiveness of RSM under the optimum conditions (40 mg/g dose of cellulase, 45 °C incubation temperature, 150 min incubation time). The final yields of pinocembrin and galangin were 2158.25 ± 0.22 μg/g and 1259.47 ± 0.14 μg/g, respectively, which are similar to the values predicted via RSM.

4. Conclusions

In this study, an efficient EP-UAS method was used for the extraction of pinocembrin and galangin from male inflorescences of *P. alba* × *berolinensis*, which was investigated via a series of single experiments and BBD to optimize the yields of pinocembrin and galangin. The obtained optimum conditions were as follows: ethanol volume fraction of 70%, cellulase dosage of 40 mg/mL, incubation temperature of 45 °C, incubation time of 150 min, pH of 5, liquid-solid ratio of 20 mL/g, duty cycle of 16.67%, ultrasound irradiation power during incubation of 200 W, ultrasound irradiation power during extraction of 200 W, and ultrasound irradiation time during extraction of 10 min. Meanwhile, the proposed EP-UAS method is a promising technique for the large-scale extraction of samples. Under the optimum conditions, the satisfactory extraction yields of pinocembrin and galangin were 2158.33 ± 0.13 μg/g and 1257.96 ± 0.06 μg/g, respectively. These experimental results indicate that the extraction yield of pinocembrin and galangin can be significantly improved under optimal conditions. The semi-pilot-scale extraction of pinocembrin and galangin was previously realized in this study, and desirable yields of pinocembrin and galangin were obtained. Despite this, the study has made some meaningful progress, but there are also some limitations, such as the stability and cost of enzyme activity, the stability of process conditions during pilot-scale expansion, and seasonal changes in raw materials. These issues need further validation and resolution in practical applications.

Supplementary Materials: The following supporting information can be downloaded at: https://www.mdpi.com/article/10.3390/separations12090249/s1, Figure S1: Diagram of the enzymatic pretreatment–ultrasonic-assisted strategy.

Author Contributions: Conceptualization, R.Z., T.L. and A.B.; Methodology, R.Z., X.L., Y.B., T.X., T.L. and A.B.; Software, R.Z., X.L., Y.B., W.X., C.X. and R.W.; Validation, Y.B., R.W. and T.X.; Formal analysis, W.X. and T.X.; Investigation, R.Z. and C.X.; Resources, X.L., W.X., C.X. and R.W.; Data curation, T.L.; Writing—original draft, R.Z. and X.L.; Writing—review & editing, T.L. and A.B.; Project administration, T.L. All authors have read and agreed to the published version of the manuscript.

Funding: This research was funded by the Natural Science Foundation of Jiangsu Province (BK20221426), the National Natural Science Foundation (32372499) and the Basic Science (Natural Science) Research Project of Jiangsu Higher Education Institution (24KJB210016).

Data Availability Statement: Data is contained within the article or Supplementary Material.

Conflicts of Interest: The authors declare no conflict of interest.

References

1. Wang, H.; Liu, H.; Wang, W.; Zu, Y. Effects of Thidiazuron, basal medium and light quality on adventitious shoot regeneration from in vitro cultured stem of *Populus alba* × *P. berolinensis*. *J. For. Res.* **2008**, *19*, 257–259. [CrossRef]
2. Bai, X.; Wang, W.; Ji, J.; Jiang, J.; Yu, Q.; Yang, C.; Liu, G. *PabCIPK24* plays an important role in the response of hybrid poplar to salt stress. *Ind. Crops Prod.* **2023**, *205*, 117452. [CrossRef]

3. Ding, C.; Zhang, W.; Li, D.; Dong, Y.; Liu, J.; Huang, Q.; Su, X. Effect of overexpression of *JERFs* on intracellular K^+/Na^+ balance in transgenic Poplar (*Populus alba* × *P. berolinensis*) under salt stress. *Front. Plant Sci.* **2020**, *11*, 1192. [CrossRef]
4. Xu, S.; He, X.; Burkey, K.; Chen, W.; Li, P.; Li, Y.; Li, B.; Wang, Y. Ethylenediurea (EDU) pretreatment alleviated the adverse effects of elevated O_3 on *Populus alba* "*Berolinensis*" in an urban area. *J. Environ. Sci.* **2019**, *84*, 42–50. [CrossRef]
5. Yu, Y.; He, R.; Chen, S.; Zhang, H.; Zhang, X.; Wang, X.; Liu, Z.; Li, Z.; Wang, Y.; Liu, W.; et al. The B-box transcription factor PabBBX27 in the regulation of chlorophyll biosynthesis and photosynthesis in poplar (*Populus alba* × *P. Berolinensis*). *Ind. Crops Prod.* **2023**, *203*, 117159. [CrossRef]
6. Zhang, Y.; Wang, B.; Jia, Z.; Scarlett, C.J.; Sheng, Z. Adsorption/desorption characteristics and enrichment of pinocembrin and galangin from *Flos populi* using macroporous resin. *Rev. Bras. Farmacogn.* **2019**, *29*, 69–76. [CrossRef]
7. Wang, B.; Goldsmith, C.D.; Zhao, J.; Zhao, S.; Sheng, Z.; Yu, W. Optimization of ultrasound-assisted extraction of quercetin, luteolin, apigenin, pinocembrin and chrysin from Flos populi by Plackett-Burman design combined with Taguchi method. *Chiang Mai J. Sci.* **2018**, *45*, 427–439.
8. Zhao, Y.; Tang, G.; Cai, E.; Liu, S.; Zhang, L.; Wang, S. Hypolipidemic and antioxidant properties of ethanol extract from Flos populi. *Nat. Prod. Res.* **2014**, *28*, 1467–1470. [CrossRef]
9. Ni, H.; Muhammad, I.; Li, J.; Wang, B.; Sheng, Z. In vitro and in vivo antioxidant activities of the flavonoid-rich extract from *Flos populus*. *Pak. J. Pharm. Sci.* **2019**, *32*, 2553–2560. [CrossRef] [PubMed]
10. Sharma, V.; Janmeda, P. Extraction, isolation and identification of flavonoid from *Euphorbia neriifo* leaves. *Arab. J. Chem.* **2017**, *10*, 509–514. [CrossRef]
11. Darwish, S.F.; Abedel Mageed, S.S.A.; Mahmoud, A.M.A.; El-demerdash, A.A.; Doghish, A.S.; Azzam, R.K.; Mohamed, R.E.; Farouk, E.A.; Noshy, M.; Shakweer, M.M.; et al. Pinocembrin protects against cisplatin-induced liver injury via modulation of oxidative stress, TAK-1 inflammation, and apoptosis. *Toxicol. Appl. Pharm.* **2025**, *502*, 117433. [CrossRef] [PubMed]
12. Li, G.; Liu, W.; Da, X.; Li, Z.; Pu, J. The natural flavonoid pinocembrin shows antithrombotic activity and suppresses septic thrombosis. *Int. Immunopharmacol.* **2024**, *142*, 113237. [CrossRef] [PubMed]
13. Hu, K.; Sun, Y.; Wang, J.; Wu, S.; Ren, J.; Su, D.; Tang, L.; Gong, J.; Fang, H.; Xu, S.; et al. Integrating network analysis and experimental validation to reveal the mechanism of pinocembrin in alleviating high glucose and free fatty acid-induced lipid accumulation in HepG2 cells. *J. Funct. Foods.* **2023**, *110*, 105879. [CrossRef]
14. Zhang, F.; Yan, Y.; Zhang, L.; Li, D.; Li, L.; Lian, W.; Xia, C.; He, J.; Xu, J.; Zhang, W. Pharmacological activities and therapeutic potential of galangin, a promising natural flavone, in age-related diseases. *Phytomedicine* **2023**, *120*, 155061. [CrossRef]
15. Wu, Y.; Luo, J.; Xu, B. Insights into the anticancer effects of galangal and galangin: A comprehensive review. *Phytomedicine* **2024**, *135*, 156085. [CrossRef]
16. Jomova, K.; Cvik, M.; Orolinova, T.; Alomar, S.Y.; Alwasel, S.H.; Aldahmash, W.; Alqarzae, S.; Al-Juaimlani, A.; Nepovimova, E.; Kuca, K.; et al. Antioxidant versus prooxidant properties of the flavonoid, galangin: ROS scavenging activity, flavonoid-DNA interaction, copper-catalyzed Fenton reaction and DNA damage study. *J. Agric. Food Res.* **2024**, *16*, 101112. [CrossRef]
17. Thapa, R.; Afzal, O.; Altamimi, A.S.A.; Goyal, A.; Almalki, W.H.; Alzarea, S.I.; Kazmi, I.; Jakhmola, V.; Singh, S.K.; Dua, K.; et al. Galangin as an inflammatory response modulator: An updated overview and therapeutic potential. *Chem.-Biol. Interact.* **2023**, *378*, 110482. [CrossRef]
18. Rampogu, S.; Gajula, R.G.; Lee, K.W. A comprehensive review on chemotherapeutic potential of galangin. *Biomed. Pharmacother.* **2021**, *141*, 11808. [CrossRef]
19. Liao, J.; Guo, Z.; Yu, G. Process intensification and kinetic studies of ultrasound-assisted extraction of flavonoids from peanut shells. *Ultrason. Sonochem.* **2021**, *76*, 105661. [CrossRef]
20. Fu, Q.; Dong, W.; Ge, D.D.; Ke, Y.; Jin, Y. Supercritical fluid-based method for selective extraction and analysis of indole alkaloids from *Uncaria rhynchophylla*. *J. Chromatogr. A* **2023**, *1710*, 464410. [CrossRef]
21. Pan, Y.; Liu, C.; Jiang, S.; Guan, L.; Liu, X.; Wen, L. Ultrasonic-assisted extraction of a low molecular weight polysaccharide from *Nostoc commune* Vaucher and its structural characterization and immunomodulatory activity. *Ultrason. Sonochem.* **2024**, *108*, 106961. [CrossRef]
22. Romero-Díez, R.; Matos, M.; Rodrigues, L.; Bronze, M.R.; Rodríguez-Rojo, S.; Cocero, M.J.; Matias, A.A. Microwave and ultrasound pre-treatments to enhance anthocyanins extraction from different wine lees. *Food Chem.* **2019**, *272*, 258–266. [CrossRef]
23. Dessie, W.; Luo, X.; Wang, M.; Liao, Y.; Li, Z.; Khan, M.R.; Qin, Z. Enhancing the valorization efficiency of Camellia oil extraction wastes through sequential green acid pretreatment and solid-state fermentation-based enzymatic hydrolysis. *Ind. Crop. Prod.* **2024**, *217*, 118893. [CrossRef]
24. Bouloumpasi, E.; Skendi, A.; Christaki, S.; Biliaderis, C.G.; Irakli, M. Optimizing conditions for the recovery of lignans from sesame cake using three green extraction methods: Microwave-, ultrasound- and accelerated-assisted solvent extraction. *Ind. Crop. Prod.* **2024**, *207*, 117770. [CrossRef]
25. Hatami, T.; Johner, J.C.F.; Meireles, M.A.A. Extraction and fractionation of fennel using supercritical fluid extraction assisted by cold pressing. *Ind. Crop. Prod.* **2018**, *123*, 661–666. [CrossRef]
26. Chemat, F.; Zill-e-Huma; Khan, M.K. Applications of ultrasound in food technology: Processing, preservation and extraction. *Ultrason. Sonochem.* **2011**, *18*, 813–835. [CrossRef]

27. Zhang, Y.; Kong, X.; Wang, Z.; Sun, Y.; Zhu, S.; Li, L.; Lv, P. Optimization of enzymatic hydrolysis for effective lipid extraction from microalgae *Scenedesmus* sp. *Renew. Energ.* **2018**, *125*, 1049–1057. [CrossRef]
28. Xu, Q.; Shen, Z.; Wang, Y.; Guo, S.; Li, F.; Wang, Y.; Zhou, C. Anti-diarrhoeal and anti-microbial activity of Flos populi (male inflorescence of *Populus tomentosa Carrière*) aqueous extracts. *J. Ethnopharmacol.* **2013**, *148*, 640–646. [CrossRef] [PubMed]
29. Ali, M.C.; Chen, J.; Zhang, H.; Li, Z.; Zhao, L.; Qiu, H. Effective extraction of flavonoids from *Lycium barbarum* L. fruits by deep eutectic solvents-based ultrasound-assisted extraction. *Talanta* **2019**, *203*, 16–22. [CrossRef] [PubMed]
30. Clardy, J.; Walsh, C. Lessons from natural molecules. *Nature* **2004**, *432*, 829–837. [CrossRef] [PubMed]
31. Chen, F.; Zhang, Q.; Liu, J.; Gu, H.; Yang, L. An efficient approach for the extraction of orientin and vitexin from *Trollius chinensis* flowers using ultrasonic circulating technique. *Ultrason. Sonochem.* **2017**, *37*, 267–278. [CrossRef]
32. Yang, X.; Liu, T.; Qi, S.; Gu, H.; Li, J.; Yang, L. Tea saponin additive to extract eleutheroside B and E from Eleutherococcus senticosus by ultrasonic mediation and its application in a semi-pilot scale. *Ultrason. Sonochem.* **2022**, *86*, 106039. [CrossRef]
33. Zhao, R.; Yang, X.; Zhang, A.; Zhou, T.; Zhou, Y.; Yang, L. An efficient approach for simultaneously obtaining oil and epigoitrin from *Orychophragmus violaceus* seeds by microwave-mediated immiscible binary solvent extraction. *Food Chem.* **2022**, *372*, 131258. [CrossRef]
34. Chen, F.; Zhang, Q.; Mo, K.; Fei, S.; Gu, H.; Yang, L. Optimization of ionic liquid-based omogenate extraction of orientin and vitexin from the flowers of *Trollius chinensis* and its application on a pilot scale. *Sep. Purif. Technol.* **2017**, *175*, 147–157. [CrossRef]
35. Wei, M.; Yang, L. Determination of orientin in *Trollius chinensis* using ultrasound- assisted extraction and high-performance liquid chromatography: Several often-overlooked sample preparation parameters in an ultrasonic bath. *J. Chromatogr. A.* **2017**, *1530*, 68–79. [CrossRef]
36. Hai, T.; Man, P.V.; Anh, L.T.H. Optimization of ultrasound-assisted extraction of astaxanthin from black tiger shrimp (*Penaeus monodon*) shells using deep eutectic solvent and ethanol as a cosolvent. *LWT* **2024**, *212*, 116965. [CrossRef]
37. Machado, T.O.X.; Kodel, H.D.A.C.; dos Santos, F.A.; dos Santos Lima, M.; Costa, A.S.G.; Oliveira, M.B.P.P.; Dariva, C.; dos Santos Estevam, C.D.; Fathi, F.; Souto, E.B. Cellulase-assisted extraction followed by pressurized liquid extraction for enhanced recovery of phenolic compounds from 'BRS Violeta' grape pomace. *Sep. Purif. Technol.* **2025**, *354*, 129218. [CrossRef]
38. Tang, Z.; Huang, G.; Huang, H. Ultrasonic/cellulase-assisted extraction of polysaccharide from Garcinia mangostana rinds and its carboxymethylated derivative. *Ultrason. Sonochem.* **2023**, *99*, 106571. [CrossRef] [PubMed]
39. Muniraj, S.; Shih, H.; Chen, Y.; Hsiech, C.; Ponnusamy, V.K.; Jen, J. Novel one-step headspace dynamic in-syringe liquid phase derivatization-extraction technique for the determination of aqueous aliphatic amines by liquid chromatography with fluorescence detection. *J. Chromatogr. A* **2013**, *1296*, 104–110. [CrossRef]
40. Wang, J.; Sun, B.; Liu, Y.; Zhang, H. Optimization of ultrasound-assisted enzymatic extraction of arabinoxylan from wheat bran. *Food Chem.* **2014**, *150*, 482–488. [CrossRef] [PubMed]
41. Romsaiyud, A.; Songkasiri, W.; Nopharatana, A.; Chaiprasert, P. Combination effect of pH and acetate on enzymatic cellulose hydrolysis. *J. Environ. Sci.* **2009**, *21*, 965–970. [CrossRef] [PubMed]
42. Zheng, F.; Yan, J.; Zhu, M.; Ye, C. Ultrasound-cellulase synergy for the extraction of total flavonoids from *Astragali complanati* Semen and its antioxidant properties. *J. Appl. Res. Med. Aroma.* **2024**, *43*, 100597. [CrossRef]
43. Fan, W.; Duan, H.; Ren, X.; Guo, X.; Zhang, Y.; Li, J.; Zhang, F.; Chen, J.; Yang, X. Optimization of ultrasound-assisted cellulase degradation method on the extraction of mulberry leaf protein and its effect on the functional characteristics. *Ultrason. Sonochem.* **2023**, *99*, 106561. [CrossRef]
44. Yang, B.; Jiang, Y.; Zhao, M.; Shi, J.; Wang, L. Effects of ultrasonic extraction on the physical and chemical properties of polysaccharides from longan fruit pericarp. *Polym. Degrad. Stabil.* **2008**, *93*, 268–272. [CrossRef]
45. Yuan, M.; Huan, X.; Yang, X.; Fan, M.; Yin, J.; Ma, Y.; Deng, B.; Cao, H.; Han, Y.; Xu, F. Simultaneous extraction of five heavy metal ions from root vegetables via dual-frequency ultrasound-assisted enzymatic digestion. *Food Chem.* **2024**, *454*, 139741. [CrossRef]
46. Wang, Z.; Wang, C.; Zhang, C.; Li, W. Ultrasound-assisted enzyme catalyzed hydrolysis of olive waste and recovery of antioxidant phenolic compounds. *Innov. Food Sci. Emerg.* **2017**, *44*, 224–234. [CrossRef]